Available online at www.sciencedirect.com

ScienceDirect

Procedia Structural Integrity 24 (2019) 810–819

Structural Integrity Procedia

www.elsevier.com/locate/procedia

AIAS 2019 International Conference on Stress Analysis

Calibration and prediction assessment of different ductile damage models on Ti6Al4V and 17-4PH additive manufactured alloys

Filippo Nalli[a,*], Andrea D'Onofrio[b], Giovanni B. Broggiato[c], Luca Cortese[c]

[a] *Faculty of Science and Technology, Free University of Bolzano-Bozen, Bolzano, Italy*
[b] *Sapienza University of Rome, Italy*
[c] *Department of Aerospace and Mechanical Engineering, Sapienza University of Rome, Italy*

Abstract

Nowadays, metal additive manufacturing is becoming always more popular, being able to deliver complex shaped high quality products. Though many studies have been conducted on the high cycle fatigue behavior of these materials, yet ductile failure has still not been completely investigated, to identify the failure limits under static complex stress states.
In the present study, the calibration of three ductile damage models on two popular additive manufactured alloys was carried out. The selected alloys were Ti6Al4V, processed via Electron Beam Melting, and 17-4PH fabricated with Selective Laser Melting technology; both broadly used in actual industrial applications. For each material a set of samples, was fabricated to perform a thorough static mechanical characterization, involving tensile tests on round smooth bars, notched bars, tests under plane strain conditions and torsion tests. The stress state in the critical points was retrieved relying on FEM simulations, and the data collected via the hybrid experimental-numerical procedure subsequently used to tune the damage models.
Specifically, the selected models are the Rice and Tracey, the Modified Mohr-Coulomb by Wierzbicki and the one proposed by Coppola and Cortese. While the former does not take into account the effect of Lode parameter, the latter two consider its influence on fracture onset. A minimization algorithm was used for their calibration, and different optimization strategies were adopted to check the robustness of identified parameters. The resulting strains to fracture as a function of damage parameters were plotted for each formulation. The failure prediction accuracy of all models was assessed and compared to the others.

Keywords: Additive manufacturing; Ductile damage models; Multiaxial tests; Structural integrity assessment

* Corresponding author. Tel.: +39 0471017734; fax: -
E-mail address: filippo.nalli@natec.unibz.it

10.1016/j.prostr.2020.02.072

1. Introduction

In mechanical design, to meet the crucial requirements of efficiency and safety, characteristics such as lightness and robustness, most of the time in contrast with each other, must be reconciled. The new additive manufacturing (AM) technologies seem to be particularly promising in being able to combine two so divergent needs, because of the possibility that they offer to produce virtually any geometry, placing the material only where necessary.

Notwithstanding the hype that these technologies are experiencing in recent years, there is still uncertainty about the actual mechanical performance of materials used in additive technologies. Numerous studies have been published recently on additive metal alloys, most of which focus on technological and process aspects (Herderick 2011), microstructure (Herzog et al. 2016) and high cycle fatigue strength (Alcisto et al. 2011; Frazier 2014). Many authors focused on the effect of heat (Fan and Feng 2018) and other post treatments (Sonntag et al. 2015), in particular Hot Isostatic Pressing (HIP) (Vrancken et al. 2012). In all cases, the static characterization was treated in a non-exhaustive manner, investigating the response of the material mostly only by conventional tensile tests.

In this scenario, the present work aims at studying the ductile behavior of two metal alloys, Ti6Al4V and 17-4PH, the first produced by Electron Beam Melting (EBM) and the latter by Selective Laser Melting (SLM). Both alloys are broadly used in actual engineering applications, as well as their wrought counterparts (not additive). The titanium alloy is mostly employed in aerospace and biomedical applications, sporting high strength but medium-low ductility; the 17-4PH is a stainless-steel alloy, showing high ductility combined with high strength.

In the paper, the authors intended to employ ductile damage models already known in the literature and profitably used for non-additive materials and prove their effectiveness in quantifying ductility and predicting fracture onset of the above mentioned AM metal alloys. At present, a very few papers have been published on the topic (Concli, Gilioli, and Nalli 2019). Different classes of ductile models are available in the literature, such as the void-growth based (Nielsen and Tvergaard 2010), the continuous damage (CDM) ones (Bonora 1997; Lemaitre 1985), or the empirical ones. The authors selected three models belonging to the last class of empirical models, for their ease of calibration on the basis of experimental evidence, thus having a strong potential in real industrial cases. Namely, the selected models were the Rice and Tracey (Rice and Tracey 1969), the one devised by Bai and Wierzbicki (Bai and Wierzbicki 2010) and the one proposed by Coppola and Cortese (Coppola, Cortese, and Folgarait 2009).

2. Materials and methods

2.1. Selected materials

The chemical composition of the investigated materials are reported in the following Table 1.

Table 1. Chemical composition of the investigated materials

Element	Ti	Al	V	C	Fe	O	N	H	Cr	Ni	Cu	Si	Mn	Nb+Ta
Ti6Al4V	Bal	6	4	0.03	0.1	0.15	0.01	0.003	-	-	-	-	-	-
17-4PH	-	-	-	0.07	Bal	-	-	-	16	4	4	1	1	0.3

Both alloys were tested without been subjected to any thermal treatment; nevertheless all specimens were machined from AM bulky parts, so that the resulting surface finishing condition is the one typical of a machining process, with $Ra < 3.2 \mu m$.

2.2. Specimen geometries and testing facilities

Samples of both materials were tested under four different loading conditions: there were executed tensile tests on smooth round bars (RB), tensile tests on notched bars with a notch radius of 10mm (RNB10), tensile tests in plane strain condition and pure torsion again on round bars. This to induce much different stress states in the

material and investigate their influence on the resulting strain at fracture. In Figure 1 the dimensions of the employed samples are reported.

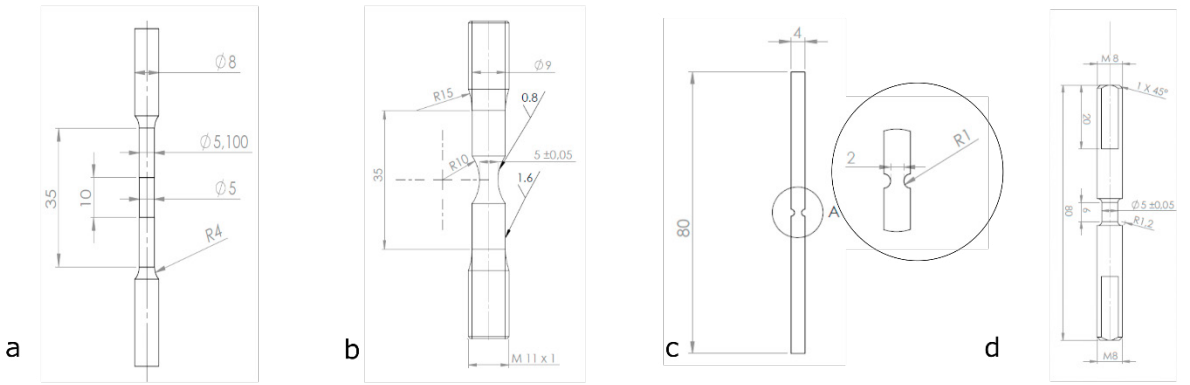

Fig. 1. Specimen geometries: (a) Round bar; (b) Round notched bar; (c) Plane strain tension; (d) Torsion.

The experiments were carried out using an MTS servo-hydraulic uniaxial tension-compression machine, and a custom made electromechanical biaxial machine, capable to apply combined tension-torsion loads at variable ratios. The testing machines are available at the Mechanical and Aerospace Department of Sapienza University of Rome. Further details on the facilities can be found in (Cortese, Nalli, and Rossi 2016).

2.3. Ductile damage models formulations

Three ductile damage models were selected: the Rice and Tracey's model, the Bai and Wierzbicki one and the damage model devised by Coppola and Cortese. For all of them ductile damage increases with the accumulation of plastic deformation, weighted on a function of the stress state (see Equation 1). Material fail as $D=1$. The models differ for the choice of the weighting function.

$$D = \int_0^{\varepsilon_f} f(\sigma) d\varepsilon_p \tag{1}$$

While for the first model only a triaxiality parameter (T) plays a role in damage accumulation, in the formulation of the latter two also the Lode parameter (X) is taken into account. These two scalar parameters are function of the invariants of the Cauchy stress tensor and their definitions are given in Equation 2.

$$T = \frac{I_1}{3\sqrt{3J_2}}; X = \frac{3\sqrt{3}}{2}\frac{J_3}{J_2^{3/2}} \tag{2}$$

I_1 is the first stress invariant, J_2 the second deviatoric stress invariant. q is the von Mises equivalent stress. Under proportional loading conditions T and X are constant and accordingly also the weighting function of Equation 1 is constant. Consequently, for each damage model, Equation 1 can be inverted, solving for ε_f, to define a fracture locus, which can be defined in a tridimensional space as a surface representing all strains to fracture corresponding to any stress state described by T, X.

The analytical expressions of the fracture locus of each adopted damage models are reported in Equation 3 (Rice and Tracey), Equation 4 (Bai and Wierzbicki), and Equation 5 (Coppola and Cortese), along with the corresponding

material constants to be calibrated.

$$\varepsilon_f = C_1 e^{C_2 T} \tag{3}$$

Where C_1 and C_2 are the parameters to be identified.

$$\varepsilon_f = \left\{ \frac{A}{C_2} \left[\sqrt{\frac{1+C_1^2}{3}} \cos\left(\frac{\pi}{6} - \vartheta \right) + C_1 \left(T + \frac{1}{3} \sin\left(\frac{\pi}{6} - \vartheta \right) \right) \right] \right\}^{-\frac{1}{n}} \tag{4}$$

C_1 and C_2 are the parameters to be calibrated, when the Von Mises yielding function is adopted.

$$\varepsilon_f = \frac{1}{C_1} e^{-C_2 T} \left(\frac{1}{\cos\left[\beta \frac{\pi}{6} - \frac{1}{3} \arccos\left(\gamma \cos(3X) \right) \right]} \right)^{\frac{1}{n}} \tag{5}$$

The parameters to be tuned in this case are C_1 and C_2 accounting for the T dependence, and γ and β, which take into account the dependence on X.

3. Experimental tests and numerical simulations

3.1. Experimental tests

All tests were run under quasi-static conditions, controlling displacement or rotation. For torsion tests, the axial actuator was held in force control, to avoid any axial load during runs (free end condition). In all tensile tests an external extensometer, with a base length of *25mm* was used. For each material and each geometry three repetitions were carried out, and the mean values of the resulting experimental curves are reported in the following Figure 2.

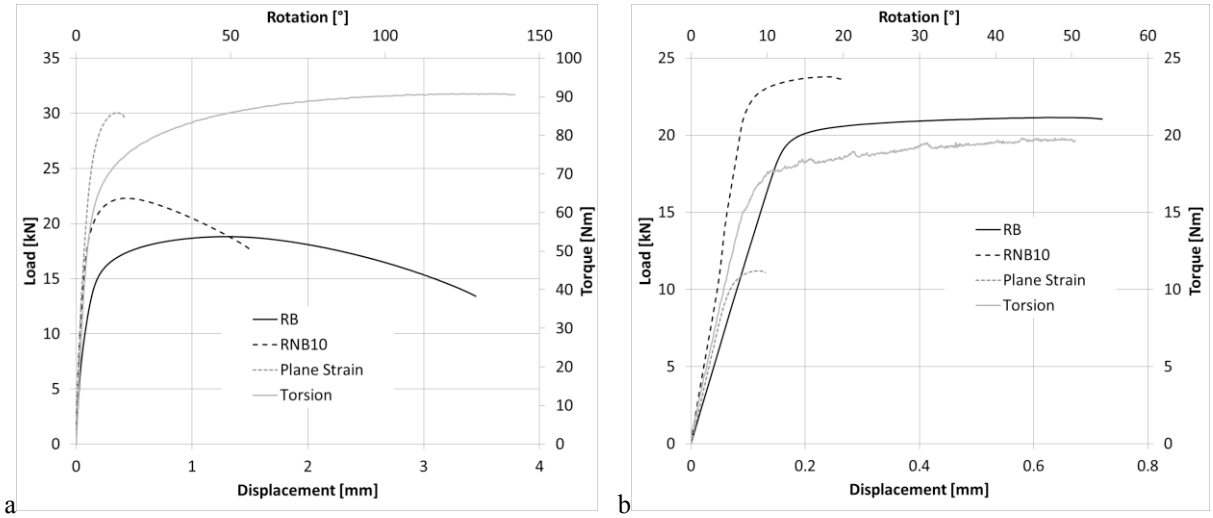

Fig. 2. (a) 17-4PH and (b) Ti6Al4V experimental force-displacement and torque-rotation curves.

3.2. Numerical simulations

For an accurate tuning of the damage models, the local stress state and the plastic deformation in the critical point through the whole loading history up to fracture must be retrieved. This task can be accomplished using numerical simulations in conjunction with a suitable material behavior, in terms of yielding criterion and subsequent plasticity evolution. Besides the simple Von Mises yielding rule, more advanced models are available (Coppola, Cortese, and Campanelli 2013; Hill 1948); in this case the classical isotropic J2 plasticity was adopted.

To retrieve the stress strain relations up to fracture, the results of the tensile tests on round smooth bars were used, calibrating the Hollomon power law ($\sigma = K\varepsilon^n$) with an inverse numerical procedure for each material. Namely, the tensile test was reproduced via FE code and the collected global force - displacement curves were compared with the experimental ones; the procedure is iterative and for each new iteration the material constitutive law was updated in the FE code, till the match between experimental and numerical global curves was satisfactory. The resulting tuned parameters of the power law are reported in Table 2, while the curves are shown in the following Figure 3.

Subsequently, each experimental test was reproduced via FEM, imposing as boundary conditions exactly the displacement or rotation ramps acquired during the experiments, up to the observed fracture; at that time the values of *T, X* and ε_f at the critical point were collected from the simulation to be used to tune the damage models.

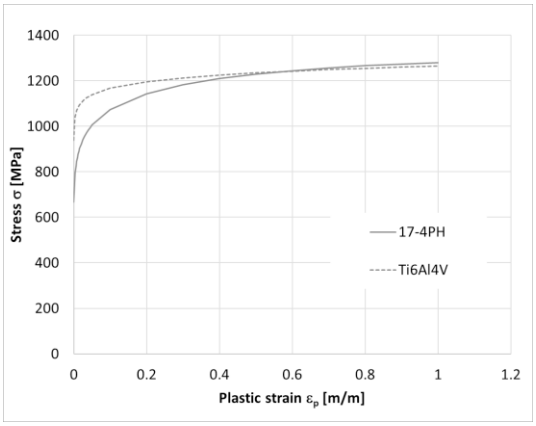

Fig. 3. True stress- true strain curves of the investigated materials, up to large strain.

Table 2. *Calibrated parameters of Hollomon power law for the investigated materials*

	K	n
17-4 PH	1360	0.1
Ti6Al4V	1265	0.035

As a matter of fact, each triplet (*T, X,* ε_f) represents a point in the tridimensional space *T, X,* ε_f through which the calibrated fracture locus should pass. To prove the effectiveness of the FE models, in Figure 4, 5 the match between numerical and experimental global curves is presented, along with a contour map of the plastic strain at fracture for each geometry tested. An even more accurate experimental – numerical comparison can be performed at local level, but requires advanced techniques, such as 3D DIC, as in (Rossi et al. 2018). In Table 3, 4 the values of the triplets (*T, X,* ε_f) for each geometry are summarized.

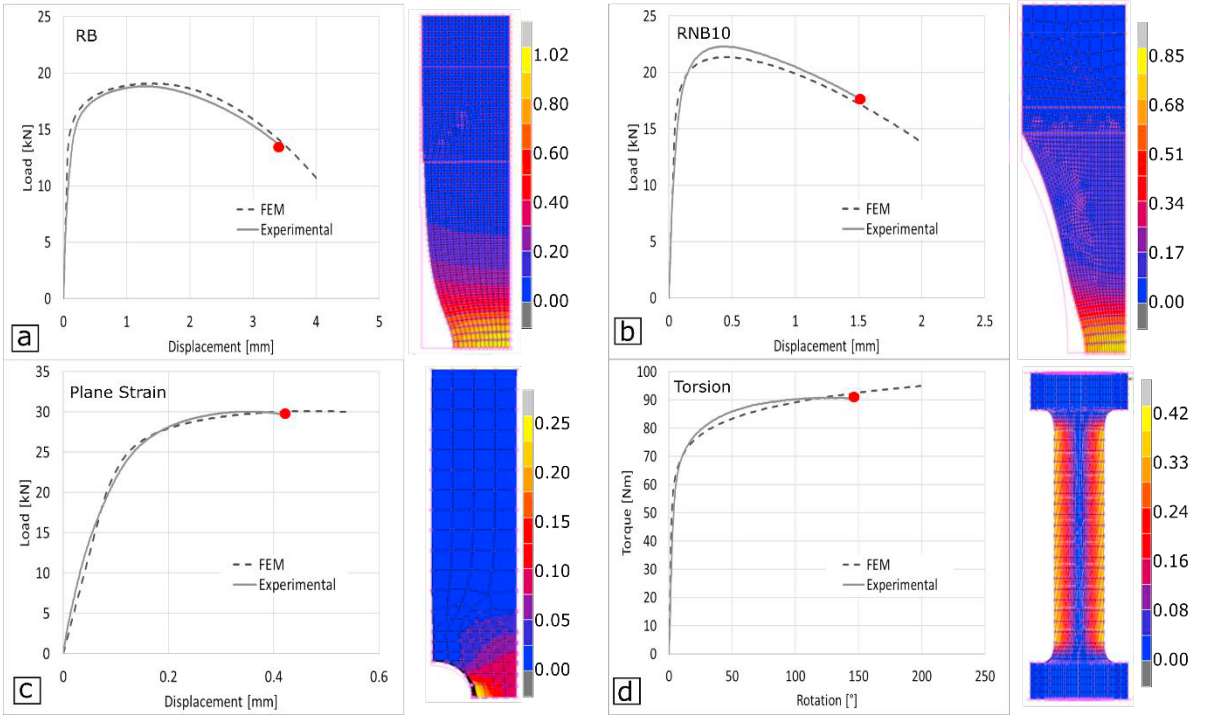

Fig. 4. Experimental – numerical match in terms of load displacement and torque rotation curves for 17-4PH: a) RB; b) RNB10; c) Plane Strain and d) Torsion

Table 3. *T, X,* ε_f values at fracture for 17-4PH

	RB	RNB10	Plane Strain	Torsion
T	0.59	0.76	0.64	0
X	0.98	0.99	0	0
ε_f	1.020	0.789	0.263	0.408

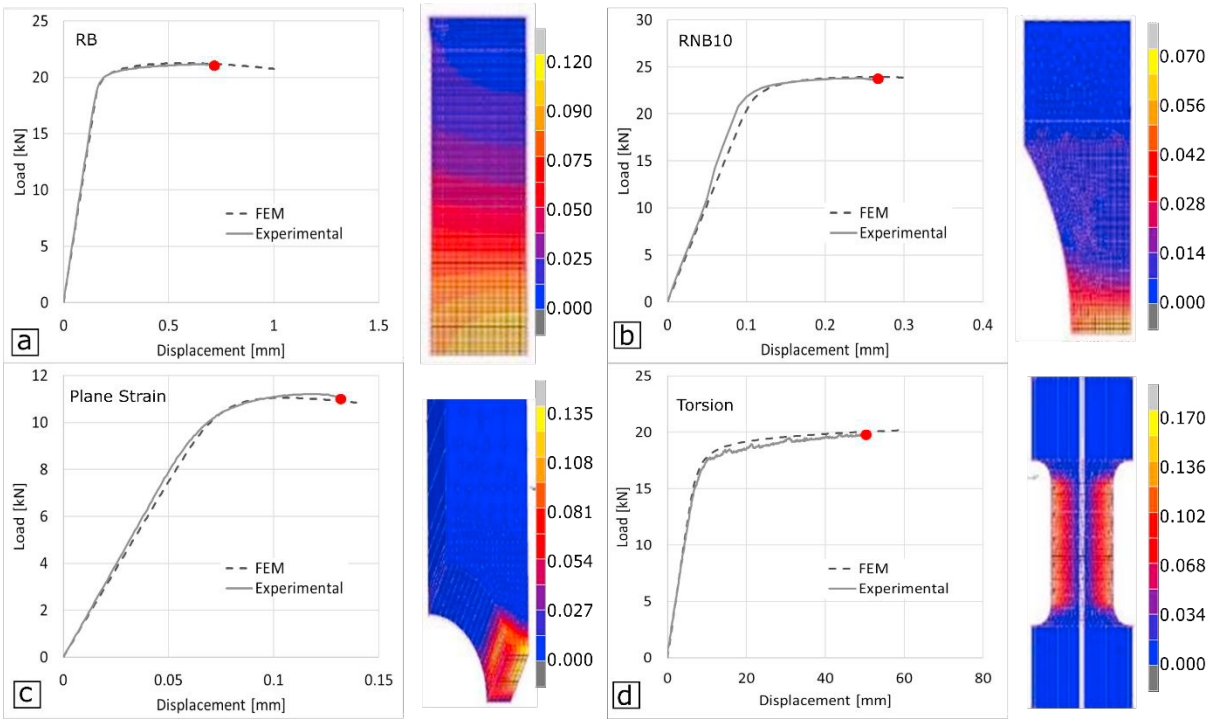

Fig. 5. Experimental – numerical match in terms of load displacement and torque rotation curves for Ti6Al4V: a) RB; b) RNB10; c) Plane Strain and d) Torsion

Table 4. *T, X*, ε_f values at fracture for Ti6Al4V

	RB	RNB10	Plane Strain	Torsion
T	0.37	0.64	0.89	0
X	1.00	0.99	0.06	0
ε_f	0.109	0.065	0.132	0.163

4. Results and discussion

4.1. Damage models tuning procedure and results

For each material, four experimental strains to fracture and corresponding stress states (*T, X*, ε_f) were retrieved from the tests (Table 3 and Table 4), to be used for the calibration of the models. To this purpose, a MATLAB routine was coded to run a constrained minimization algorithm, in order to find the best fit fracture locus surface matching the four experimental points, for each damage model. The routine accepts as input the four points coordinates and gives back the values of the tuned parameters of the chosen model. Figures 6a), 6b) and 6c) show the calibrated fracture surfaces for 17-4PH, while the subsequent Figures 7a), 7b) and 7c) report the surfaces tuned for Ti6Al4V.

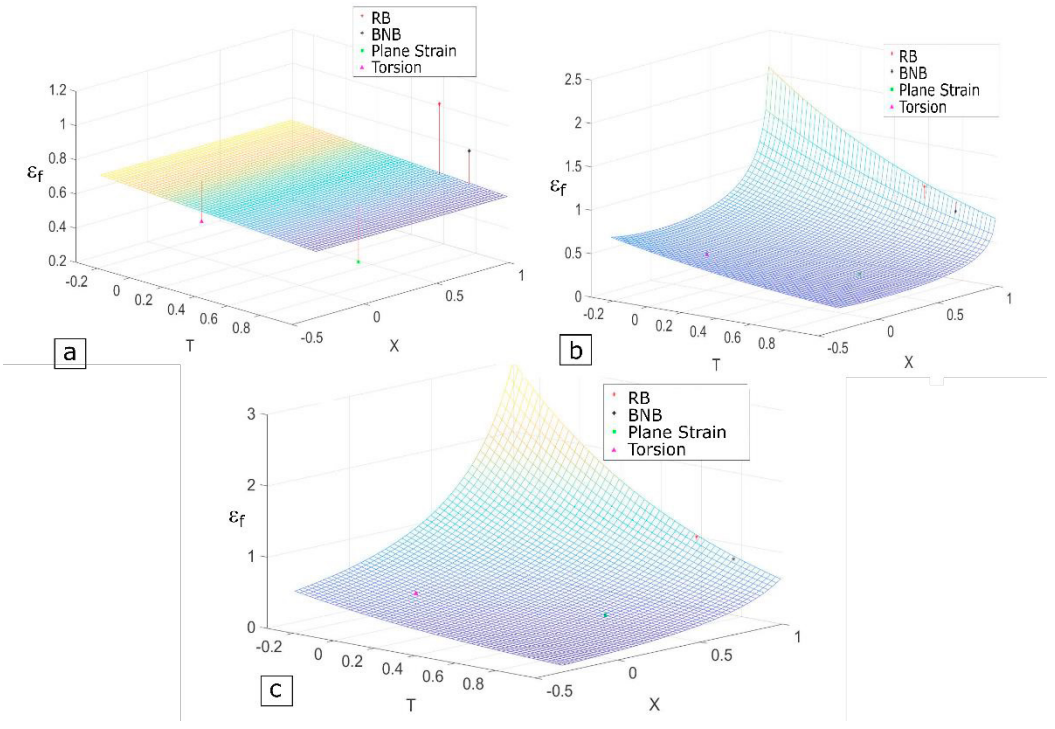

Fig. 6. Ductile damage model fracture surfaces, calibrated for 17-4PH: a) Rice and Tracey; b) Bai and Wierzbicki; c) Coppola and Cortese

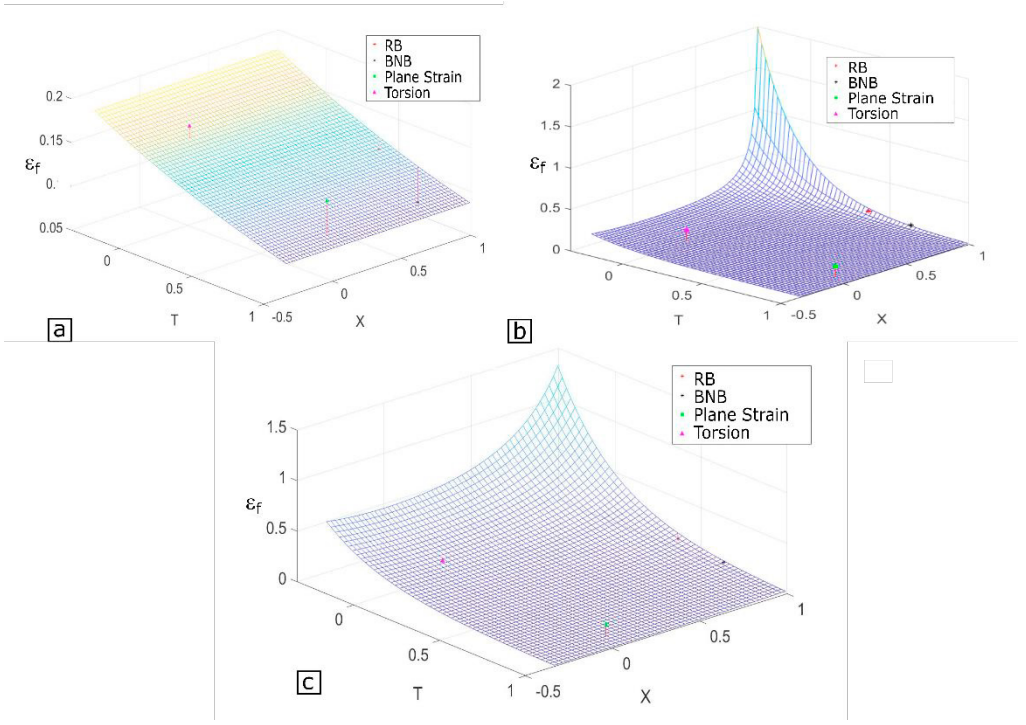

Fig. 7. Ductile damage model fracture surfaces, calibrated for Ti6Al4V: a) Rice and Tracey; b) Bai and Wierzbicki; c) Coppola and Cortese

A critical analysis of the presented results shows that the Rice and Tracey model, though broadly used in the past decades, cannot meet the experimental strain to fractures of all four tests concurrently. This is due to the effect of the Lode parameter X on fracture, which is not considered by the model formulation. On the other hand, the Bai and Wierzbicki and the Coppola and Cortese models, once calibrated, seem to capture the experimental strains to fracture with good approximation. This is a first evidence that these two ductile damage models can be used successfully also for AM materials. It is worth pointing out that the tuned fracture loci of the two models differ one another far from the points used for calibration. This implies that their overall prediction accuracy may differ. Having available more experimental strain to fracture points, corresponding to additional different stress states could lead to a more robust calibration.

4.2. Assessment of fracture prediction accuracy

The percentage difference between experimental and numerical strain to fracture was used for a more quantitative prediction accuracy assessment of each damage model. In the following Tables 5, 6 the percentage errors are summarized.

Table 5. Experimental-numerical strain at fracture error for 17-4PH

Percentage error	RB	RNB10	Plane Strain	Torsion
Rice Tracey	43.7	29.7	-115	-58.2
Wierzbicki	21.6	.3.48	-7.69	0.68
Coppola Cortese	4.32	-4.87	-8.32	2.11

Table 6. Experimental-numerical strain at fracture error for Ti6Al4V

Percentage error	RB	RNB10	Plane Strain	Torsion
Rice Tracey	-2.08	-38.7	44.4	8.26
Wierzbicki	-3.83	27.9	98.9	82.9
Coppola Cortese	-45.2	10.5	92	6

From Tables 5, 6 it comes out that for 17-4PH the errors of the Bai and Wierzbicki and Coppola and Cortese models are very low and comparable, thus confirming that these models can be advantageously used with this alloy. Instead, for Ti6Al4V errors are higher, such that the models should be used with caution. The difference can be attributed to the much lower ductility of Ti6Al4Vwith respect to 17-4PH, with strains at fracture not much different one another (see the last row of Table 4). This behavior is typical of semi-brittle materials; it is then natural that models which were devised for quite ductile materials perform worse on materials which exhibit a very limited ductility.

5. Conclusions

A thorough static characterization was carried out on additive manufacturing structural 17-4PH and Ti6Al4V alloys, executing multiaxial tests to induce highly differentiated stress states in the material. Numerical simulations of each test were performed to retrieve the data needed for the damage models calibration. Three ductile damage models, one accounting only for triaxiality effect, the other two taking into account also the dependence on Lode parameter, were tuned for each material. A fracture prediction capability analysis was carried out, showing that the

models including the Lode parameter influence could be profitably used on AM metal alloys. Also, it was found that the accuracy of the models was strongly related to the overall ductility of the materials, with a consistent better prediction for the highly ductile ones.

Acknowledgements

The authors wish to thank prof. Giuseppe Mirone, for his valuable contribution and for providing part of the samples. The research was partially funded by Free University of Bolzano – Bozen with the grant number TN2092 "Additive manufacturing for advanced functional design".

References

Alcisto, J., A. Enriquez, H. Garcia, S. Hinkson, T. Steelman, E. Silverman, P. Valdovino, H. Gigerenzer, J. Foyos, J. Ogren, J. Dorey, K. Karg, T. McDonald, and O. S. Es-Said. 2011. "Tensile Properties and Microstructures of Laser-Formed Ti-6Al-4V." *Journal of Materials Engineering and Performance* 20(2):203–12.

Bai, Y. and T. Wierzbicki. 2010. "Application of Extended Mohr-Coulomb Criterion to Ductile Fracture." *International Journal of Fracture* 161(1):1–20.

Bonora, N. 1997. "A Nonlinear CDM Model for Ductile Failure." *Engineering Fracture Mechanics* 58(1/2):11–28.

Concli, F., A. Gilioli, and F. Nalli. 2019. "Experimental–Numerical Assessment of Ductile Failure of Additive Manufacturing Selective Laser Melting Reticular Structures Made of Al A357." *Proceedings of the Institution of Mechanical Engineers, Part C: Journal of Mechanical Engineering Science* 0(0):1–8.

Coppola, T., Luca Cortese, and F. Campanelli. 2013. "Implementation of a Lode Angle Sensitive Yield Criterion for Numerical Modelling of Ductile Materials in the Large Strain Range." Pp. 1097–1108 in *Computational Plasticity XII: Fundamentals and Applications - Proceedings of the 12th International Conference on Computational Plasticity - Fundamentals and Applications, COMPLAS 2013*.

Coppola, T., Luca Cortese, and P. Folgarait. 2009. "The Effect of Stress Invariants on Ductile Fracture Limit in Steels." *Engineering Fracture Mechanics* 76(9):1288–1302.

Cortese, Luca, F. Nalli, and M. Rossi. 2016. "A Nonlinear Model for Ductile Damage Accumulation under Multiaxial Non-Proportional Loading Conditions." *International Journal of Plasticity* 85:77–92.

Fan, Z. and H. Feng. 2018. "Study on Selective Laser Melting and Heat Treatment of Ti-6Al-4V Alloy." *Results in Physics* 10(July):660–64.

Frazier, E. W. 2014. "Metal Additive Manufacturing: A Review." *Journal of Materials Engineering and Performance* 23(6):1917–28.

Herderick, E. 2011. "Additive Manufacturing of Metals: A Review." *Materials Science and Technology Conference and Exhibition 2011* 2(176252):1413–25.

Herzog, D., V. Seyda, E. Wycisk, and C. Emmelmann. 2016. "Additive Manufacturing of Metals." *Acta Materialia* 117:371–92.

Hill, R. 1948. "A Theory of Yielding and Plastic Flow of Anisotropic Metals." *Proceedings of the Royal Society of London. Series A, Mathematical and Physical Sciences*.

Lemaitre, J. 1985. "A Continuum Damage Mechanics Model for Ductile Fracture." *Journal of Engineering Materials and Technology* 107:83–89.

Nielsen, K. L. and V. Tvergaard. 2010. "Ductile Shear Failure or Plug Failure of Spot Welds Modelled by Modified Gurson Model." *Engineering Fracture Mechanics* 77(7):1031–47.

Rice, J. R. and D. M. Tracey. 1969. "On the Ductile Enlargement of Voids in Triaxial Stress Fields*." *Journal of the Mechanics and Physics of Solids* 17(3):201–17.

Rossi, M., Luca Cortese, K. Genovese, A. Lattanzi, F. Nalli, and F. Pierron. 2018. "Evaluation of Volume Deformation from Surface DIC Measurement." *Experimental Mechanics* 58(7):1181–94.

Sonntag, R., J. Reinders, J. Gibmeier, and J. P. Kretzer. 2015. "Fatigue Performance of Medical Ti6Al4V Alloy after Mechanical Surface Treatments." *PLoS ONE* 10(3):1–15.

Vrancken, B., L. Thijs, J. P. Kruth, and J. Van Humbeeck. 2012. "Heat Treatment of Ti6Al4V Produced by Selective Laser Melting: Microstructure and Mechanical Properties." *Journal of Alloys and Compounds* 541:177–85.